The role of nonlinear critical layers in boundary layer transition

By M. E. Goldstein

National Aeronautics and Space Administration, Lewis Research Center Cleveland, OH 44135, USA

Asymptotic methods are used to describe the nonlinear self-interaction between pairs of oblique instability modes that eventually develops when initially linear spatially growing instability waves evolve downstream in nominally two-dimensional laminar boundary layers. The first nonlinear reaction takes place locally within a so-called 'critical layer', with the flow outside this layer consisting of a locally parallel mean flow plus a pair of oblique instability waves – which may or may not be accompanied by an associated plane wave. The amplitudes of these waves, which are completely determined by nonlinear effects within the critical layer, satisfy either a single integro-differential equation or a pair of integro-differential equations with quadratic to quartic-type nonlinearities. The physical implications of these equations are discussed.

1. Introduction

Transition to turbulence in boundary layers usually begins with initially linear and non-interacting instability waves that grow to nonlinear amplitudes as they propagate downstream. The first nonlinear stage of evolution (which might more appropriately be referred to as a modal-interaction stage) is usually characterized by the rapid growth of three-dimensional disturbances due to resonant interactions between instability waves and between instability waves and streamwise vortices. This phenomenon is usually studied experimentally by artificially exciting the flow with small-amplitude nearly-two-dimensional and single-frequency excitation devices. The initial unsteady motion just downstream of the excitation device should then have harmonic time dependence and be well described by linear instability theory. In most cases, the mean flow is relatively two dimensional and fairly close to a Blasius profile in the low Mach-number experiments and to the corresponding compressible flow in the high Mach-number experiments. (There are actually very few controlled excitation experiments at high Mach numbers, but there is some hope that this will change in the near future.) The instability-wave growth rates should therefore be small compared to the inverse boundary-layer thickness Δ^{-1} at subsonic Mach numbers, but can be of the same order as Δ^{-1} at sufficiently high supersonic Mach numbers (due to the generalized mean-flow inflection point that occurs in this case). However, mean-flow divergence effects will usually cause the growth rate to be small (relative to Δ^{-1}) by the time nonlinear effects set in, even in these more unstable supersonic flows. This is because, in the latter type of flows, the excitation is usually located in the vicinity of the peak local growth rate of the relevant normalized instability growth-rate versus frequency curve – such as the one shown schematically

Phil. Trans. R. Soc. Lond. A (1995) **352**, 425–442
Printed in Great Britain

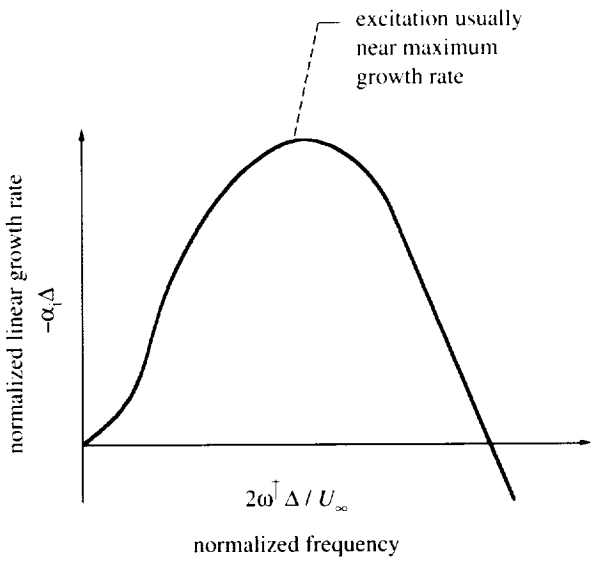

Figure 1. Typical linear growth-rate curve.

in figure 1. The growth rate should therefore decrease as the (constant frequency) instability wave propagates downstream into a region where (in most cases) the boundary-layer thickness Δ will have increased.

This suggests that the method of matched asymptotic expansions can be used to describe these flows: with an 'inner' nonlinear region, in which the instability-wave growth rate is small, and a much larger 'outer' region in which the unsteady flow is governed by linear dynamics, but in which mean-flow divergence effects are important (Goldstein & Leib 1988). Once the solutions in these two regions have been found, a uniformly valid composite solution that applies everywhere in the linear and nonlinear regions can be obtained in one of the usual ways – say, by multiplying the linear and nonlinear solutions together and then dividing through by their common part in the overlap domain (that always exists between the inner and outer regions).

Smoke wires and other flow-visualization devices can be used to observe the flow when the Mach number is sufficiently small. The initial nonlinear (or modal-interaction) stage then becomes visible through the appearance of rows of Λ-shaped structures, which can either be aligned or staggered in alternating rows – depending on the experimental conditions. The unstaggered arrangement, which was originally observed by Klebanoff & Tidstrom (1959) and Klebanoff *et al.* (1962), is usually referred to as 'peak-valley' splitting (or K-type transition). It is (as pointed out by Kachanov & Levchenko (1984, § 5.2)) a complex phenomena that is explainable by at least three different (relatively weak) resonant-type interaction mechanisms – each of which probably played some role in one or more of the many experiments that have been carried out to study this phenomena (see Kachanov *et al.* 1985; Kachanov 1987; Hama & Nutant 1963; Kovasznay *et al.* 1962; Nishioka *et al.* 1979). A resonant-type interaction between oblique instability waves and weak streamwise vortices seems to have played a dominant role in the original experiments of Klebanoff & Tidstrom (1959) and Klebanoff *et al.* (1962). However, Stewart & Smith (1992) propose a different mechanism that seems to be in good agreement with experimental observations.

The staggered arrangement, which tends to predominate at the lower excitation levels, is usually associated with a weak nonlinearity resulting from a resonant-triad

interaction between a pair of oblique subharmonic modes (which, in most cases, originated from the background disturbance environment) with the basic fundamental two-dimensional mode generated by the excitation device. This type of interaction was originally analysed for Tollmien–Schlichting-type (i.e. viscous-type) instabilities by Craik (1971) and subsequently by many others who used finite Reynolds-number-type approaches and recently by Smith & Stewart (1987) who used asymptotic methods. (However, see Khokhlov (1994*a*) and the discussion section of Wu *et al.* (1994).) Moreover, there are now a number of carefully controlled experiments (Kachanov *et al.* 1977; Kachanov & Levchenko 1984; Saric & Thomas 1984; Saric *et al.* 1984; Coke & Mangano 1989) that basically verify the resonant-triad mechanism, but the observed growth rates tend to be much smaller than those predicted by the finite Reynolds-number theories (Khokhlov 1994*b*).

Craik (1971) proposed that the resonant-triad interaction could also play a role in the aligned or K-type transition, but with the interaction taking place between a pair of oblique modes at the forcing frequency and the small two-dimensional instability mode that is invariably generated at the first harmonic of this frequency (see § 5.2 of Kachanov & Levchenko (1984) for a more complete discussion of this issue). All of the relevant modes could then be generated by the excitation device and would not have to emanate from the background disturbance environment. However, the analysis could not predict the observed gradual transition from a two- to a three-dimensional flow structure unless the (common) amplitude of the oblique modes were able to exceed that of the two-dimensional fundamental and, consequently, that of the (usually much smaller) first harmonic that causes the enhanced growth of the oblique modes. This behaviour would obviously be favoured if the oblique modes were unable to suppress the growth of the first harmonic until they themselves became very large because this would allow the oblique modes to continue their rapid growth until they became larger than the more slowly growing two-dimensional mode generated at the forcing frequency. As shown below, the present high-Reynolds-number theory actually exhibits this behaviour. In any event, this latter mechanism probably played an important role in the recent peak-valley splitting experiments of Kachanov (1987) and Kachanov *et al.* (1985) but may not have been very significant in the original Klebanoff experiments.

2. The outer linear flow

We first consider the initial linear region just downstream of the excitation device where the instability waves are still small enough so that no significant modal interactions take place. At supersonic Mach numbers below about 6 or so where the so-called first-mode instability is dominant (Mack 1984, 1987), the most rapidly growing modes are oblique instability waves, and the first modal interaction to take place would probably be the self-interaction between symmetric pairs of oblique instability waves (Leib & Lee 1994). In which case, it is appropriate to suppose that the unsteady motion is initiated from a pair of oblique (equi-amplitude) instability-wave modes with the same streamwise wave number α_r and scaled angular frequency $\omega^\dagger \Delta / U_\infty = \alpha_r c_r$ and equal and opposite spanwise wave numbers ($\pm\beta$). (U_∞ is the characteristic velocity of the flow, and the subscript r is used to denote the real part of the wave number α and the phase speed c, as well as all other quantities to which it is appended.) These two waves combine to form a standing wave in the spanwise direction that propagates only in the direction of flow which is the situation that

most frequently occurs in wave excitation experiments that typically involve longish excitation devices placed perpendicular to the flow.

The two-dimensional mode usually† exhibits the most rapid growth at subsonic speeds provided, of course, that the mean flow is sufficiently two dimensional. However, even very weak spanwise periodic mean-flow distortions (i.e. streamwise vortices) can cause appropriate oblique modes to grow faster than the plane wave at the high Reynolds numbers being considered herein. This could occur, for example (Goldstein & Wundrow 1994), through a kind of resonant-interaction mechanism that was first considered by Nayfeh (1981) and Nayfeh & Al-Maaitah (1988) and later applied to Görtler vortices by Hall & Seddougui (1989). In which case it would again be appropriate to initiate the unsteady motion from a pair of oblique waves of the type described above — but with the growth rates equal to the parametric growth rates given in Goldstein & Wundrow (1994). But, even when no streamwise vortices are present (or when they are very weak) and the mean flow is effectively two dimensional, the oblique modes can eventually exhibit the most rapid growth due to a parametric resonant interaction with the plane wave that exhibits the most rapid growth in the initial linear stage. The oblique modes can then become large enough to interact themselves nonlinearly upon passing through the parametric resonance interaction stage, which can be treated simultaneously with the self-interaction stage if we initiate the unsteady motion from a resonant triad of instability waves in the initial linear region — a plane fundamental-frequency wave, with scaled angular frequency $2\omega^{\dagger}\Delta/U_{\infty}$, and a pair of oblique equi-amplitude subharmonic waves, (again) with the same streamwise wave number and angular frequency, α_{r} and $\alpha_{\mathrm{r}}c_{\mathrm{r}}$, respectively, and equal but opposite spanwise wave numbers $\pm\beta$. In this case, the term 'resonance' implies, among other things, that the three waves all have the same phase speed c_{r}. This occurs (for the small growth rates and large Reynolds numbers that are of interest here) when

$$\beta = \sqrt{3}\alpha_{\mathrm{r}}, \tag{2.1}$$

which means that the oblique instability waves make a 60° angle with the direction of flow. We can, of course, allow this angle to be arbitrary in flows where an oblique mode can grow more rapidly than the plane wave and resonant reaction with the latter is not required to enhance the growth rate of the former.

Our choice of the initial linear modes may, at first, seem somewhat artificial, but the linear and parametric resonance stages act as narrow band filters that are able to select out these disturbances from relatively generic background disturbance fields. Moreover, we eventually show (at the end of § 3) that the resonance condition (2.1) does not have to be satisfied exactly and that the results actually apply to a fairly broad range of wave numbers about the resonant condition.

It is only possible to develop a systematic asymptotic theory of these phenomena when the Reynolds number Re is assumed to be large. Then, since we also require that the instability-wave growth rates be small in the nonlinear region of the flow, the initial modal and nonlinear interactions will be confined to a localized region centred around the 'critical level' (Lin 1951), where the mean-flow velocity, say U_{c}, is equal to the common phase velocity c_{r} of the two or three modes that interact there (see figure 2). This occurs because the flow must be nearly steady in a reference frame moving downstream with the phase velocity c_{r} at the small growth rates being

† Stewart & Smith (1987) show that non-parallel flow effects can sometimes cause the oblique modes to grow faster than the two-dimensional mode.

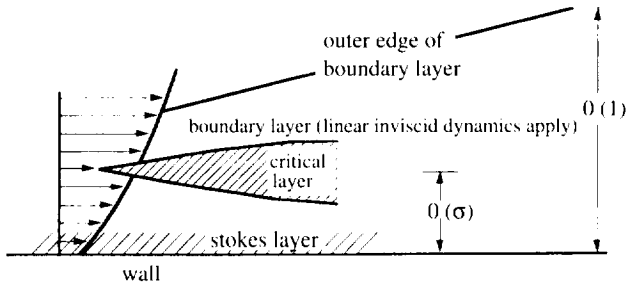

Figure 2. Asymptotic structure of flow.

considered herein, and, the corresponding mean flow is then equal to zero at the critical layer by definition. There is, therefore, no mean flow to linearize the analysis about in this region, and the nonlinear and/or modal interaction effects will then come into play at the lowest possible order of approximation there. This explains why energy exchange between resonant modes (which share a common critical layer) is much more efficient than between non-resonant modes.

The flow outside the 'critical layer' is still governed by linear dynamics, which means that it is either (*a*) still given by a locally parallel two-dimensional streamwise mean flow, say $U(y)$, or perhaps (in the case where the wavelength scale factor α is $\ll 1$) a nearly two-dimensional streamwise mean flow, say $U(y)+\sigma^4 U_0(y, 2Z)$, plus a pair of oblique instability-wave modes or (*b*) is given by a locally parallel mean flow $U(y)$ plus a pair of oblique instability modes accompanied by a first harmonic plane (i.e. two-dimensional) instability wave. The (external) transverse velocity fluctuation v is then given (in the general compressible case) by

$$v = \epsilon\sigma\bar{\alpha}\,\mathrm{Re}[\sec\theta A(x_0)\Phi(y)\mathrm{e}^{\mathrm{i}X}\cos Z + (\epsilon/\sigma)^{1/3}A_0(x_0)\Phi_0(y)\mathrm{e}^{\mathrm{i}2X}], \tag{2.2}$$

where

$$X = \sigma\bar{\alpha}(x - \sigma\bar{c}t), \quad Z = \sigma\bar{\beta}z, \tag{2.3}$$

$$\left.\begin{aligned} \alpha = \sigma\left[\bar{\alpha} + 0\left(\frac{\epsilon}{(1+\lambda)\sigma}\right)^{1/3}\right], \quad c = \sigma\left[\bar{c} + 0\left(\frac{\epsilon}{(1+\lambda)\sigma}\right)^{1/3}\right], \\ c_0 = \sigma\left[\bar{c} + 0\left(\frac{\epsilon}{(1+\lambda)\sigma}\right)^{1/3}\right], \end{aligned}\right\} \tag{2.4}$$

$$x_0 = \sigma(\epsilon/\sigma)^{1/3}x, \tag{2.5}$$

the scale factor $\sigma \leqslant 1$ has to be inserted in order to simultaneously cover the $O(1)$ and long-wavelength cases, $\theta = \tan^{-1}(\bar{\beta}/\bar{\alpha})$, and Re denotes the real part. The streamwise, transverse and spanwise coordinates, normalized by the boundary-layer thickness Δ, are x, y and z, respectively; t denotes the normalized time, and θ denotes the propagation angle of the oblique mode (which is equal to $\frac{1}{3}\pi$ when the oblique modes are resonant with the plane wave, but is otherwise arbitrary). The scaled spanwise wave number, streamwise wave number and phase speed $\bar{\beta}$, $\bar{\alpha}$ and $\bar{c}$, respectively, are purely real.

The first term on the right-hand side of equation (2.2) represents the oblique modes, while the second term represents the plane wave. Φ and Φ_0 are the linear normal-mode shapes which can, in general, be found by solving the appropriate Rayleigh's equation (but see below). A and A_0, which depend only on the streamwise

coordinate (and then only through the scaled streamwise variable x_0, which varies on the length scale of the nonlinear region which, not very surprisingly, turns out to be the reciprocal instability-wave growth rate) determine the overall growth of the instability waves and are, therefore, the most important quantities in these equations. They are completely determined by the nonlinear dynamics within the critical layer and are, in practice, found by equating the velocity jump across the critical layer, as calculated from the external linear solution (i.e. the solution to Rayleigh's equation) to the velocity jump calculated from the internal nonlinear solution within the critical layer. ϵ and $\epsilon(\epsilon/\sigma)^{1/3}$ are the amplitude scale factors for the oblique and plane waves, respectively, where ϵ is always much less than σ.

Notice that the growth-rate and oblique-mode amplitude scalings $\sigma(\epsilon/\sigma)^{1/3}$ and ϵ, respectively, are related. This relation ensures that linear growth and nonlinear (or modal interaction) effects will both impact the external linear solution at the same asymptotic order. It is dictated by the requirement that the nonlinear stage correspond to the first stage of evolution beyond the initial linear region, i.e. that the nonlinear solutions match onto the upstream linear solutions in the matched asymptotic sense. The Benney–Bergeron (1969) parameter $\lambda \equiv 1/\epsilon\sigma^3 Re$, where Re is the Reynolds number based on the boundary layer thickness Δ, is (in the present context) a measure of the relative importance of viscous to growth-rate effects within the critical layer, i.e. these effects will be of the same order when $\lambda = O(1)$.

The wavelength scale factor σ can be set to unity when the initial linear instability wave has order-one wavelength – as is usually the case in supersonic flows with sufficiently high Mach numbers. Then the linear instability-wave growth rate will be $O(\epsilon^{1/3})$ (Goldstein & Choi 1989) as the nonlinear region is approached (which fixes the location of this region).

For the asymptotically more stable flows, such as subsonic boundary layers with sufficiently small adverse-pressure gradients ($= O(\sigma^2)$) or with sufficiently weak spanwise mean-flow distortions, σ will be small compared to unity, and the linear growth rate will scale like σ^4 over most of the unstable region (Goldstein & Lee 1992; Wundrow *et al.* 1994; Goldstein & Wundrow 1994). The nonlinear critical-layer effects will therefore come into play over most of the unstable region (and not just near the neutral curve) if we take

$$\sigma(\epsilon/\sigma)^{1/3} = \sigma^4, \quad \text{when } \lambda = O(1), \quad \sigma(\epsilon/\lambda\sigma)^{1/3} = \sigma^4, \quad \text{when } \lambda \to \infty. \tag{2.6}$$

And for even more stable flows, such as accelerating boundary layers (Reid 1965; Wu 1993) with $O(1)$ pressure gradients, the growth rate will be $O(\sigma^2)$ over the main part of the unstable region. In which case, the nonlinear critical-layer effects will come into play in the major portion of this region if we take

$$(\epsilon/\lambda\sigma)^{1/3} = \sigma, \quad \text{as } \lambda \to \infty. \tag{2.7}$$

Finally, we note that the phase speeds of the oblique and plane-wave modes, c and c_0, respectively, will only be equal (i.e. resonance will only occur) if $\bar{\alpha}$ and $\bar{\beta}$ satisfy (2.1), or equivalently if α and β satisfy (2.1) to within order $\sigma(\epsilon/(1+\lambda)\sigma)^{1/3}$.

3. Critical layer dynamics and the amplitude equations

The lowest-order critical-layer equations turn out to be linear and (in the most general case) correspond to a balance between growth (i.e. non-equilibrium), mean-flow convection and viscous-diffusion effects. The nonlinear and modal interaction effects

are weak in the present description, which means that they do not affect the lowest order equations, but enter only through inhomogeneous terms in a higher-order problem. This ultimately implies that the scaled oblique-mode amplitude function A can be determined from a single amplitude equation or that the amplitude functions A and A_0 can be determined from a pair of amplitude equations – depending on whether or not the parametric resonance stage plays a role in the interaction. In the former case, the relevant equation corresponding to the generalized scaling (2.3) through (2.5) is given by Goldstein & Choi (1989), Wu *et al.* (1993), Goldstein & Wundrow (1994) and Leib & Lee (1994) as

$$\frac{\mathrm{d}\tilde{A}}{\mathrm{d}\tilde{x}} = \tilde{\kappa}\tilde{A} + \mathrm{i}\tilde{\gamma}\int_{-\infty}^{\tilde{x}}\int_{-\infty}^{x_1}\tilde{K}_\theta\tilde{A}(x_1)\tilde{A}(x_2)\tilde{A}^*(x_1+x_2-\tilde{x})\,\mathrm{d}x_2\,\mathrm{d}x_1, \tag{3.1}$$

and, in the latter case, are given by Goldstein & Lee (1992, 1993), Wu (1992), Goldstein (1994) and Mallier & Maslowe (1994) as

$$\begin{aligned}\frac{\mathrm{d}\tilde{A}(\tilde{x})}{\mathrm{d}\tilde{x}} = {} & \tilde{\kappa}\tilde{A}(\tilde{x}) + \mathrm{i}\int_{-\infty}^{\tilde{x}} K_0\tilde{A}_0(x_1)\tilde{A}^*(2x_1-\tilde{x})\,\mathrm{d}x_1 \\ & + \mathrm{i}\tilde{\gamma}\int_{-\infty}^{\tilde{x}}\int_{-\infty}^{x_1}\tilde{K}_{\pi/3}\tilde{A}(x_1)\tilde{A}(x_2)\tilde{A}^*(x_1+x_2-\tilde{x})\,\mathrm{d}x_2\,\mathrm{d}x_1,\end{aligned} \tag{3.2}$$

$$\begin{aligned}\frac{\mathrm{d}\tilde{A}_0(\tilde{x})}{\mathrm{d}\tilde{x}} = {} & \tilde{\kappa}_0\tilde{A}_0(\tilde{x}) + \mathrm{i}\tilde{\rho}\tilde{\gamma}\int_{-\infty}^{\tilde{x}}\int_{-\infty}^{x_1}[K_1\tilde{A}_0(x_1)\tilde{A}(x_2) \\ & \times\tilde{A}^*(2x_1+x_2-2\tilde{x}) + K_2\tilde{A}(x_1)\tilde{A}_0(x_2)\tilde{A}^*(x_1+2x_2-2\tilde{x})]\,\mathrm{d}x_2\,\mathrm{d}x_1 \\ & + \mathrm{i}\tilde{\rho}\tilde{\gamma}^2\int_{-\infty}^{\tilde{x}}\int_{-\infty}^{x_1}\int_{-\infty}^{x_2}K_3\tilde{A}(x_1)\tilde{A}(x_2)\tilde{A}(x_3) \\ & \times\tilde{A}^*(x_1+x_2+x_3-2\tilde{x})\,\mathrm{d}x_3\,\mathrm{d}x_2\,\mathrm{d}x_1,\end{aligned} \tag{3.3}$$

where the asterisks denote complex conjugates; $\tilde{x}$, $\tilde{A}$ and $\tilde{A}_0$ are suitably renormalized, and shifted variables corresponding to x_0, A, and A_0, respectively; and $\tilde{\rho}$ and $\tilde{\gamma}$ are complex parameters which are dependent on the basic mean flow. The real parameter $\tilde{\kappa}$ represents the linear growth rate of the oblique mode, or the resonant growth rate of this mode when there is a sufficiently strong spanwise distortion of the mean flow. The real part of $\tilde{\kappa}_0$ is the scaled linear growth rate of the plane wave. Its imaginary part $\tilde{\kappa}_0$, $\tilde{\kappa}_{0\mathrm{i}}$, accounts for the initial wave-number shift between the oblique and plane-wave modes.

Notice that these are integro-differential equations of the type first proposed for Rossby waves by Hickernell (1984), rather than the usual ordinary differential equations of the classical Stuart–Watson–Landau (Landau & Lifshitz 1987) theory. The integrals arise from upstream history effects that produce a gradual phase shifting between modes when the nonlinearity takes place within a non-equilibrium (or growth-dominated) critical layer. This occurs because the evolution or growth effects have a dominant (i.e. first-order) effect on the flow within the critical layer, but only weakly affect the flow outside the critical layer. The nonlinear (or wave-interaction) terms are therefore influenced by the growth effects when they are generated within the critical layer, but not when they are generated outside the critical layer, as in the classical Stuart–Watson–Landau theory.

The nonlinear kernel functions $\tilde{K}_\theta$, K_0 and K_1–K_3 will be discussed subsequently.

They turn out to be simple polynomial functions of the streamwise (and corresponding integration) variables in the inviscid limit $\lambda \to 0$, and in the general case involve integrals of exponentials and polynomials of the streamwise coordinates. $\tilde{K}_\theta$ explicitly depends on the obliqueness angle θ and $\tilde{K}_{\pi/3} \equiv \tilde{K}_{\theta=\pi/3}$.

Classical Stuart Watson Landau theory suppresses the critical-layer effects which can only be justified when the Reynolds number is assumed to be sufficiently small. For inviscidly unstable boundary layers, this assumption is inconsistent with the locally parallel flow approximation (Huerre 1980; Huerre 1987; Goldstein & Leib 1988; Goldstein & Hultgren 1988). For high-Reynolds-number viscously unstable boundary layers, classical weakly nonlinear theory is restricted to a rather smallish region in the vicinity of the lower branch of the neutral stability curve – in which case the size of the upstream linear region would have to be extremely small. Moreover, nonlinearity usually occurs in the vicinity of the upper branch of the neutral stability curve in most of the relevant boundary-layer experiments (Mankbadi *et al.* 1993).

To be consistent with our requirement that the solutions evolve from an initially linear stage, the amplitude equations (3.1) or (3.2) and (3.3) usually have to be solved subject to the upstream boundary conditions

$$\tilde{A} \to a^{(0)} e^{\tilde{\kappa}\tilde{x}}, \quad \tilde{A}_0 \to e^{\tilde{\kappa}_0 \tilde{x}}, \quad \text{as } \tilde{x} \to -\infty. \tag{3.4}$$

so that they match onto the linear small growth-rate solution far upstream, or that they match onto the appropriate resonant growth-rate solution when spanwise distortion effects play a role – however, see §6 below for an important exception to this. Notice that only the first term on each of the right-hand sides of equations (3.2) and (3.3) contributes to these equations when $\tilde{A}$ and $\tilde{A}_0$ are sufficiently small – as they are initially – and that (3.4) is then an exact solution to the resulting equations.

We include the linear wave-number shift $\tilde{\kappa}_{0i}$ to allow for an appropriate amount of wave-number detuning in the analyses, which means that resonance (2.1) does not necessarily have to be exact and that the analysis actually applies to a relatively broad wave-number range about this resonance condition. And even more generally, we could modify equations (3.1) (3.3) to include wave-packet effects, as in Huerre (1980), Smith & Stewart (1987), Smith & Bowles (1992) and Wu *et al.* (1994) – but in the interest of simplicity, we do not pursue this issue here.

When applied, for example, to adverse-pressure-gradient boundary layers, the solutions to equations (3.2) and (3.3) are not uniformly valid in frequency as $\Delta\omega^\dagger/U_\infty \to 0$. This is because there is a viscous Stokes layer at the wall that eventually contributes a term

$$\frac{(\sigma\bar{c})^3 U_c'^2}{(\epsilon/\sigma)^{1/3}[2\,Re(2\omega^\dagger \Delta/U_\infty)^5]^{1/2}},$$

where U_c' is the Blasius skin friction, to the scaled linear growth rate $\tilde{\kappa}_0$ when $\Delta\omega^\dagger/U_\infty$ becomes sufficiently small. However, the relevant solutions can easily be made uniformly valid for all frequencies (except in the immediate vicinity of the lower branch) by simply replacing the relevant linear growth rates ($\tilde{\kappa}$ and $\tilde{\kappa}_0$ in equations (3.2) and (3.3), respectively) by

$$\left.\begin{aligned} \tilde{\kappa} &\to \tilde{\kappa} + \frac{4}{5}\frac{(\sigma\bar{c})^3 U_c'^2}{(\epsilon/\sigma)^{1/3}[Re(2\omega^\dagger \Delta/U_\infty)^5]^{1/2}}, \\ \tilde{\kappa}_0 &\to \tilde{\kappa}_0 + \frac{(\sigma\bar{c})^3 U_c'^2}{(\epsilon/\sigma)^{1/3}[2\,Re(2\omega^\dagger \Delta/U_\infty)^5]^{1/2}}. \end{aligned}\right\} \tag{3.5}$$

4. The mean-flow change

A significant feature of the present high-Reynolds-number approach is that the nonlinear critical-layer interaction produces a spanwise-variable mean-flow change

$$u = \epsilon \operatorname{Re} \bar{u}_0(y, x_0)\mathrm{e}^{2iZ}, \tag{4.1}$$

that is of the same order as the oblique-mode instability wave (see equation (2.2)) that initially produces the interaction. However, the associated cross-flow velocities

$$v = \sigma\epsilon(\epsilon/\sigma)^{1/3} \operatorname{Re} \bar{v}_0\mathrm{e}^{2iZ}, \quad w = \epsilon(\epsilon/\sigma)^{1/3} \operatorname{Re} \bar{w}_0\mathrm{e}^{2iZ} \tag{4.2}$$

turn out to be somewhat smaller than this.

In the remainder of the paper, we discuss the implications of the fundamental equations (3.1) (3.3).

5. The pure oblique-mode interaction

We begin by considering the case where only the oblique modes enter into the interaction. We have seen that this situation is relevant to supersonic boundary layers and to subsonic flows with sufficiently strong streamwise vortices. It should therefore be highly relevant to the original Klebanoff *et al.* (1962) experiment (i.e. K-type transition).

The common oblique-mode amplitude is now determined by equation (3.1). Its kernel function $\tilde{K}_\theta$ is relatively complicated when viscous effects are retained, as in Wu *et al.* (1993), but in the inviscid limit originally considered by Goldstein & Choi (1989) and Goldstein & Wundrow (1994), it is simply

$$\tilde{K}_\theta = -\tfrac{1}{2}\tan^2\theta\cos 2\theta(\tilde{x} - x_1)[(\tilde{x} - x_1)^2 + (\tilde{x} - x_2)^2 - \cos 2\theta(\tilde{x} - x_2)(x_1 - x_2)], \tag{5.1}$$

provided that $\sigma \ll 1$ in the case where streamwise vortices play a role. Wundrow & Goldstein (1994) also considered the streamwise vortex problem in the order-one wavelength, i.e. the $\sigma = 1$ limit. They show that the instability-wave amplitude is still given by (3.1), provided the nonlinear kernel functions is taken to be a slight generalization of (5.1).

$\tilde{K}_\theta$ vanishes when $\theta = \frac{1}{4}\pi$, and the inviscid solution to (3.1) develops a singularity at a finite downstream position (Goldstein & Choi 1989), say x_s, at all other angles. $\tilde{A}$ therefore exhibits explosive growth at $\tilde{x}_s$, with the local asymptotic behavior being given by (Goldstein & Choi 1989; Shukhman 1991)

$$\tilde{A} \sim \frac{a}{(\tilde{x}_s - \tilde{x})^{3+i\phi}}, \quad \text{as } \tilde{x} \to \tilde{x}_s, \tag{5.2}$$

where the real parameters a and ϕ are related to the original parameters $\tilde{\kappa}$ and $\tilde{\gamma}$ through quadratures. Figure 3 is a plot of the scaled amplitude function versus the scaled streamwise coordinate, as calculated numerically from equations (3.1) and (5.1) for $\tilde{\alpha} = 1.2$ and various values of θ. The curves show that the solution initially follows the linear growth corresponding to

$$\frac{\mathrm{d}\tilde{A}}{\mathrm{d}\tilde{x}} = \tilde{\kappa}\tilde{A}, \tag{5.3}$$

and that the explosive growth occurs very suddenly once nonlinearity comes into play. The dashed curves are the local asymptotic expansions calculated from equation (5.2). This result implies that the overall wave-number/growth-rate scaling is

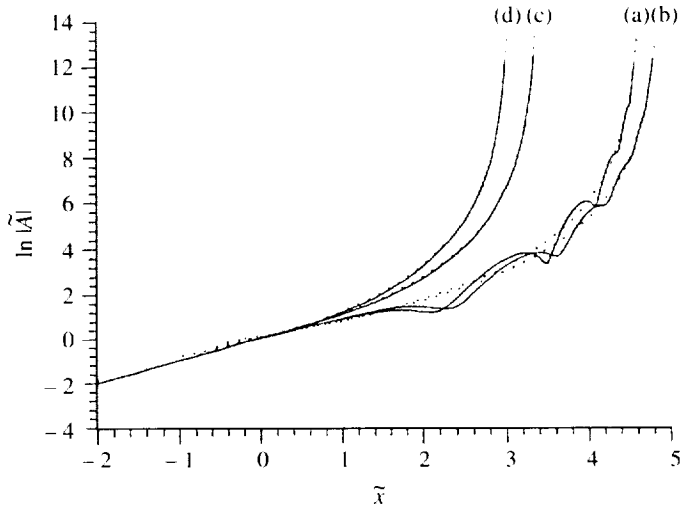

Figure 3. A plot of the scaled amplitude against the scaled streamwise coordinate: (*a*) $\theta = 15°$; (*b*) $\theta = 30°$; (*c*) $\theta = 60°$; (*d*) $\theta = 75°$. Solid lines: numerical solutions; dotted lines: local asymptotic solutions (from Wu *et al.* 1993).

preserved right up to the singularity when $\sigma = 1$, which means that the overall asymptotic structure remains intact until the instability-wave amplitude becomes $O(1)$ everywhere in the flow, and that the motion is then governed by the full nonlinear Euler equations in the next stage of evolution.

However, the growth-rate amplitude scaling is not preserved in the long wavelength limit $\sigma \to 0$ (corresponding to, say, the weak streamwise vortex-amplification mechanism). In this case, the critical layer expands to fill the inviscid wall layer that surrounds the critical layer, causing the flow to become fully nonlinear while the instability amplitudes are still small. The next stage of evolution is then characterized by a three-layer structure and is governed by the three-dimensional unsteady 'triple-deck' equations, but without the viscous terms (Goldstein & Lee 1992). This does not, however, imply that the relevant scaling is the usual triple-deck scaling in this stage.

Wu *et al.* (1993) showed that explosive growth also occurs in the viscous case and that the local asymptotic behaviour in the vicinity of the singularity is still given by (5.2). However, they also showed that (as in Goldstein & Leib (1989) and Leib (1991)) there is a certain range of parameters where explosive growth does not occur when the viscous parameter λ exceeds a certain (usually very large) value. The instability wave will then reach a peak amplitude at some fixed streamwise location and subsequently undergo viscous decay downstream of that point.

6. The parametric resonance interaction

Now suppose that the scaled oblique-mode amplitude A is very small and remains that way during the entire resonant interaction. Notice that this includes the case $A = O(\epsilon/\sigma)^{1/3}$, where the oblique mode has the same amplitude scaling as the plane wave (as was originally pointed out by Goldstein & Lee 1992).

The last term can be neglected on the right-hand side of equation (3.2), which

then becomes

$$\frac{\mathrm{d}\tilde{A}}{\mathrm{d}\tilde{x}} = \tilde{\kappa}\tilde{A} + \mathrm{i}\int_{-\infty}^{\tilde{x}} K_0 \tilde{A}_0(x_1)\tilde{A}^*(2x_1 - \tilde{x})\,\mathrm{d}x_1. \tag{6.1}$$

while the plane-wave amplitude equation (3.3) reduces to the linear growth-rate equation

$$\frac{\mathrm{d}\tilde{A}_0}{\mathrm{d}\tilde{x}} = \tilde{\kappa}_0\tilde{A}_0, \tag{6.2}$$

which merely reflects the fact that there is no back reaction of the oblique mode on the plane wave. It may seem rather surprising that this occurs even when the oblique-mode amplitude is much larger than that of the plane wave, but the critical-layer velocity jump that would produce back reaction at this level turns out to be identically zero. It is worth noting that the back-reaction effects would have to be quadratic in the oblique-mode amplitudes if they occurred at the equi-amplitude stage.

Since the second member of the oblique-mode equation (6.1) is now linear in $\tilde{A}$, we refer to it as the parametric resonance term. Its kernel function, which was first given in Goldstein & Lee (1993), is

$$K_0 = \tfrac{3}{2}(\tilde{x} - x_1)^2 \exp(-\tfrac{2}{3}\bar{\lambda}(\tilde{x} - x_1)^3), \tag{6.3}$$

where $\bar{\lambda}$ is a suitably renormalized parameter corresponding to λ. Goldstein & Lee (1992) give an analytical solution to (6.1) through (6.3) for the inviscid limit $\bar{\lambda} = 0$ and Wundrow *et al.* (1993) extend it to the viscous case where $\bar{\lambda} = O(1)$. These solutions show that the oblique-mode instability-wave amplitude can be represented by an infinite series of terms each of which exhibits exponential growth. They also show that $\tilde{A}$ tends to be dominated by the lower-order terms at small values of $\tilde{x}$, but that the higher modes rapidly come into play and the 'infinite tail' of the series eventually determines the behaviour of the solution at large values of $\tilde{x}$. This leads to the conclusion that

$$\tilde{A} \sim c_0 \exp(\tfrac{1}{2}\mathrm{i}\arg \mathrm{i}\tilde{A}_0)\exp(\tilde{\kappa}_{0\mathrm{r}}\tilde{x}/5)\exp\left(\int_{-\infty}^{\tilde{x}_0}(\tfrac{1}{4}\tilde{A}_0)^{1/4}\,\mathrm{d}\tilde{x}\right), \quad \text{as } \tilde{x} \to \infty, \tag{6.4}$$

provided that the shifting of the coordinate is correct to $O(\sigma)$ in the long-wavelength limit, where $\sigma \ll 1$ and $\tilde{\kappa} = \frac{4}{5}\tilde{\kappa}_0$. Here, $\tilde{x}_0$ is a shifted coordinate corresponding to $\tilde{x}$, c_0 is a real constant, and $\tilde{A}_0$ is given by equation (6.2).

Notice that K_0 (as given by equation (6.3)) becomes highly concentrated around $\tilde{x} = x_1$ in the strongly viscous limit:

$$\bar{\lambda} \to \infty, \quad \text{with } \hat{\kappa} \equiv \lambda^{1/3}\tilde{\kappa} = O(1). \tag{6.5}$$

Equation (6.1) therefore reduces to the ordinary differential equation

$$\frac{\mathrm{d}\hat{A}}{\mathrm{d}\hat{x}} = \hat{\kappa}\hat{A} + \tfrac{3}{4}\mathrm{i}\hat{A}_0\hat{A}^*, \tag{6.6}$$

where

$$\hat{x} = \bar{\lambda}^{-1/3}\tilde{x}, \quad \hat{A} = \bar{\lambda}^{-1/3}\tilde{A}, \quad \text{and} \quad \hat{A}_0(\tilde{x}) \equiv \bar{\lambda}^{-2/3}\tilde{A}_0. \tag{6.7}$$

The limit (6.5) corresponds to (among other things) the flat plate or Blasius boundary layer, i.e. the flow in which the resonant-triad interaction was first analysed by Craik (1971). In fact, equation (6.6) is within a constant factor of the equation obtained by

Craik (1971), who used conventional Stuart–Watson–Landau theory (Stuart 1960; Watson 1960; Landau & Lifshitz 1987) together with finite Reynolds-number-type arguments to derive his result. The corresponding limiting form of the general plane-wave amplitude equation (3.3) is still the linear equation (6.2).

Virtually all subharmonic transition experiments have been carried out in flat-plate boundary layers with very-low free-stream Mach numbers so that the Blasius boundary-layer solution provides an appropriate description of the mean flow. The amplitude/growth-rate scaling for linear instability waves in the major portion of the unstable Reynolds-number range is then given by equation (2.6) and as shown, for example, by Bodonyi & Smith (1981) and Goldstein *et al.* (1986), $Re = O(\sigma^{-10})$ and $2\omega^{\dagger}\Delta/U_{\infty} = O(\sigma^{2})$ in this range. In which case, it follows from equation (2.6) and the definition of λ that $\epsilon = \epsilon\sigma^{10}$ and $\bar{\lambda} = \sigma^{-3/2}$, and, therefore (in view of equation (6.5)), that both terms on the right-hand side of equation (3.5) are of the same order. This scaling is valid at all sufficiently large Reynolds numbers including those corresponding to the upper branch of the neutral stability curve. Mankbadi *et al.* (1993) point out that the initial parametric resonant interaction first becomes significant in the vicinity of (and in some cases downstream of) the upper branch in virtually all subharmonic transition experiments carried out to date. They also note that it occurs at relatively small values of the frequency parameter $2\omega^{\dagger}\Delta/U_{\infty}\,Re = \sigma^{12}$ presumably because, as theory suggests, the relative strength of this interaction increases with decreasing σ. The present asymptotic theory, which holds at small values of σ, should therefore provide a reasonable description of this phenomenon.

The classical high-Reynolds-number asymptotic solution for the upper branch of the neutral stability curve (Reid 1966) is the relevant solution in the initial linear and non-interacting stage. This solution is basically inviscid except for a thin viscous wall layer and a relatively thin critical layer which is asymptotically distinct from the wall layer. The lowest-order critical-layer equation corresponds to a balance between mean-flow convection and viscous diffusion effects.

As in the general case discussed above, the first modal interactions occur within the critical layer once the linear plane-wave amplitude becomes sufficiently large, but since the lowest-order critical-layer equations now correspond to a balance between linear convection and viscous diffusion effects, the oblique instability-wave amplitude is determined by the viscous critical-layer amplitude equation (6.6). However, this equation, together with equation (6.2), shows that the oblique-mode growth rate $(\mathrm{d}\hat{A}/\mathrm{d}\hat{x})/\hat{A}$ continues to increase as the instability waves propagate downstream, so that the non-equilibrium (or growth) effects, which are missing in the lowest-order critical-layer equations, must eventually come into play — causing equation (6.6) to become invalid.

In fact, equations (6.2), (6.6) and (6.7) imply that (Craik 1971; Wundrow *et al.* 1993)

$$\hat{A} \sim \hat{C}_0 \exp(\mathrm{i}\pi/4) \exp\left(\hat{\kappa}\hat{x} + \frac{3}{4\hat{\kappa}_{0\mathrm{r}}} \exp(\hat{\kappa}_{0\mathrm{r}}\hat{x})\right), \quad \text{as } \hat{x} \to \infty, \tag{6.8}$$

where $\hat{C}_0$ is a real constant: we have chosen the origin of the coordinates so that

$$\hat{A}_0 = \exp(\hat{\kappa}_{0\mathrm{r}}\hat{x}), \tag{6.9}$$

and, for simplicity, we assume that $\hat{\kappa}$ is real.

Notice that equation (6.8) does not reduce to the limiting form of equation (6.4) as $\bar{\lambda} \to \infty$, which means that the limits $\bar{\lambda} \to \infty$ and $\tilde{x} \to \infty$ cannot be interchanged and,

consequently, that there must be some intermediate solution that connects asymptotic solutions (6.4) and (6.8). In fact, Wundrow *et al.* (1993) show that approximation (6.6) becomes invalid when $\hat{\kappa}\hat{x} = O(\ln \bar{\lambda}^{2/3})$ and that the non-equilibrium effects become of the same order as the viscous effects for larger values of $\hat{x}$, at which point the flow begins to evolve on the faster scale

$$\bar{x} = \bar{\lambda}^{1/3}\left(\tilde{x} - \frac{1}{\tilde{\kappa}_{0\mathrm{r}}}\ln \bar{\lambda}^{2/3}\right) = \bar{\lambda}^{2/3}\hat{x}_1, \tag{6.10}$$

where

$$\hat{x}_1 \equiv \hat{x} - \frac{1}{\hat{\kappa}_{0\mathrm{r}}}\ln \bar{\lambda}^{2/3} \tag{6.11}$$

is an appropriately shifted coordinate on the $\hat{x}$-scale, and the oblique-mode amplitude is determined by the fully non-equilibrium equation (6.1), but with $\hat{A}_0(\hat{x})$ treated as a slowly varying function of $\tilde{x}$ and the linear growth term treated as a higher-order effect. The relevant solution has the WKBJ form (Goldstein 1994)

$$\bar{A} = C_0 \exp(\mathrm{i}\pi/4)\sqrt{\frac{b'}{b}}b^q \exp(\bar{\lambda}^{2/3})\int_0^{\hat{x}_1} b(\xi)\,\mathrm{d}\xi, \tag{6.12}$$

where the prime denotes differentiation with respect to $\hat{x}$, $q = \tilde{\kappa}/\tilde{\kappa}_0$, b is determined by the transcendental equation

$$b(\hat{x}_1) = \tfrac{3}{2}\hat{A}_0(\hat{x}_1)\int_0^{\infty} \exp(-\tfrac{2}{3}\zeta^3 - 2b(\hat{x}_1)\zeta)\zeta^2\,\mathrm{d}\zeta, \tag{6.13}$$

$$\bar{A} \equiv \frac{1}{\bar{\lambda}}\tilde{A}, \tag{6.14}$$

and C_0 is a real constant.

Notice that $\hat{A}_0 \to 0$, $b \to \frac{3}{4}\hat{A}_0$ and, consequently, that

$$\bar{A} \to C_0(\tfrac{3}{4})^q\sqrt{\hat{\kappa}_{0\mathrm{r}}}\exp(\mathrm{i}\pi/4)\exp\left(\hat{\kappa}\hat{x}_1 + \frac{3}{4}\frac{\bar{\lambda}^{2/3}}{\hat{\kappa}_{0\mathrm{r}}}(\exp(\hat{\kappa}_{0\mathrm{r}}\hat{x}_1) - 1)\right), \quad \text{as } \hat{x}_1 \to -\infty, \tag{6.15}$$

which means that the solution (6.12) will match onto the asymptotic expansion (6.8) of the solution to the viscous-limit equation (6.6) if we take

$$\hat{C}_0 = \sqrt{\hat{\kappa}_{0\mathrm{r}}}C_0(\tfrac{3}{4}\bar{\lambda}^{1/6})^q \exp\left(\frac{-3\bar{\lambda}^{(2/3)}}{4\hat{\kappa}_{0\mathrm{r}}}\right). \tag{6.16}$$

This shows that the critical-layer dynamics are eventually controlled by non-equilibrium (or growth-rate) effects, even in the Blasius boundary layer, and that the uniformly valid solution for the instability-wave amplitude is ultimately determined by non-equilibrium equation (6.1) and not by the viscous-limit equation (6.6).

Figure 4 is a plot of the oblique-mode growth rate as calculated from the full non-equilibrium equation (6.1) for various values of the nearly constant scaled plane-wave amplitude $\tilde{A}_0$. The straight line is the result obtained from viscous limit equation (6.6). Notice that the non-equilibrium growth rates are consistently lower then the corresponding equilibrium values, which might, as pointed out by Khokhlov (1994), just explain the discrepancy between the growth rates predicted by the classical Craik-type theories and those observed experimentally.

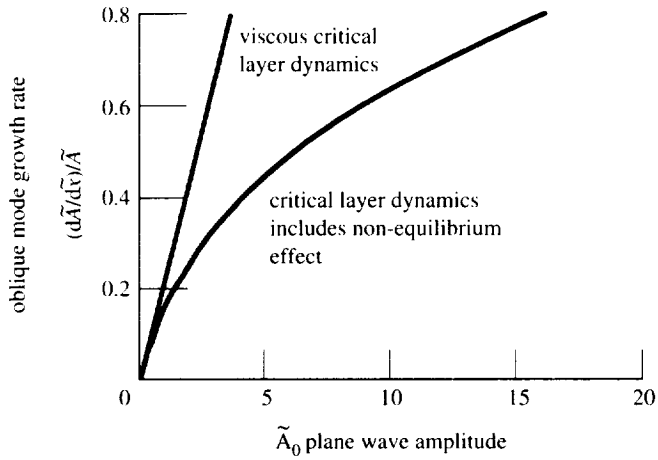

Figure 4. Oblique mode growth rate as a function of scaled plane-wave amplitude. (Prepared by Dr Sang Soo Lee.)

7. The full resonant-triad interaction

Equations (6.12) and (6.13) show that the oblique mode continues to grow (when $\bar{A}_0$ is given by equation (6.2)) and must therefore eventually become large enough to not only react back on the plane wave but also interact nonlinearly with itself. The plane wave and oblique mode will then both evolve on the faster scale $\bar{x}$ as defined in equation (6.10).

The simplest way to show this is to notice that the viscous parameter $\bar{\lambda}$ can be scaled out of the general equations (3.2) and (3.3) by introducing the scaled dependent and independent variables (6.10), (6.14), along with $\bar{A}_0 \equiv A_0/\bar{\lambda}^{4/3}$, and then replacing the linear growth rates $\tilde{\kappa}$ and $\tilde{\kappa}_0$ by the scaled growth rates $\tilde{\kappa}/\bar{\lambda}^{1/3}$ and $\tilde{\kappa}_0/\bar{\lambda}^{1/3}$, respectively. Then, aside from the vanishing of the linear growth terms, the resulting equations will remain unchanged in the limit $\bar{\lambda} \to \infty$, with $\hat{\kappa}$ (as defined by equation (6.5)) and the barred variables held fixed. These latter equations do not possess solutions that satisfy the linear upstream boundary conditions (3.4), but they do possess solutions that satisfy the alternative conditions

$$\bar{A} \to \bar{a}^{(0)} \exp(\mathrm{i}\pi/4) \exp(b_0 \bar{x}), \quad \bar{A}_0 \to 1, \quad \text{as } \bar{x} \to -\infty, \tag{7.1}$$

where

$$b_0 \equiv \tfrac{3}{2} \int_0^\infty \zeta^2 \exp(-\zeta^3 - 2b_0\zeta)\, \mathrm{d}\zeta, \tag{7.2}$$

and therefore match onto the $\hat{x}_1 \to 0$ limit of the parametric resonance solution (6.12) and (6.13) and the linear plane-wave solution $\bar{A}_0 \equiv \exp(\hat{\kappa}_0 \hat{x}_1)$.

The previous results show that these latter solutions match onto an intermediate viscous parametric resonance stage (which is governed by equation (6.6)) and, consequently, onto the same upstream boundary conditions as equations (6.9) and (6.6) (i.e. equation (3.4) with the $\tilde{}$ replaced by $\hat{}$) provided, of course, that

$$\bar{a}^{(0)} = O(\bar{\lambda}^{q/6} \exp(-3\bar{\lambda}^{2/3}/4\hat{\kappa}_{0\mathrm{r}})).$$

This means that the fully interactive stage will be governed by the full non-equilibrium equations (3.2) and (3.3) if the oblique modes are exponentially smaller than the plane wave at the start of resonance even in the Blasius boundary layer.

The smaller linear growth rate of the oblique modes could easily cause this situation to occur – even when all the modes have the same amplitude at the start of the linear stage.

We now return to the general resonant-triad equations (3.2) and (3.3). The significance of the various terms in equation (3.2) has already been discussed. The relevant kernel functions are given by (5.1) and (6.3). However, we have not, as yet, discussed the nonlinear terms in equation (3.3). They account for the back reaction of the oblique mode on the plane wave – with the first group representing a kind of mutual interaction. The relevant kernel functions are given by Goldstein & Lee (1992) and Mallier & Maslowe (1994) in the inviscid limit, and by Wu (1994) in the general case.

The last term in equation (3.3), which is quartic in the oblique-mode amplitudes, does not involve the plane-wave amplitude at all. The early, i.e. finite Reynolds-number-type, analyses of the resonant-triad interaction (see, for example, Craik (1971) and other references) involve a corresponding back-reaction term that is, however, only quadratic in the oblique mode amplitudes. The kernel function for this last term (of equation (3.3)) is also given by Goldstein & Lee (1992) and Mallier & Maslowe (1994) in the inviscid limit and by Wu (1994) in the general case.

8. Concluding remarks

In most boundary layer flows, it is the oblique-mode instability waves that ultimately exhibit the most rapid growth – either directly from the initial linear stage or indirectly through an intermediate parametric resonance stage. The cubic self-interaction between the oblique-mode instability waves is one of the first strictly nonlinear interactions to come into play as the instability waves evolve downstream in such flows. This interaction can have a dominant effect on the subsequent instability-wave development – producing a local singularity (and consequently explosive growth) at a finite downstream position in the inviscid limit and sometimes producing viscous decay when viscosity is present (Goldstein 1994; Wu 1993).

The more or less general case is described by equation (3.1), or by equations (3.2) and (3.3), but depending on the initial amplitude ratio and the external parameters, various limiting forms of these equations can apply to different regions of the flow giving rise to a wide variety of different phenomena. The nonlinear interaction also produces a spanwise variable mean-flow change in the linear region outside the critical layer. It is of the same order as the oblique-mode instability waves in the inviscid case, but can be even larger than these in the strongly viscous case (Goldstein 1994).

The author thanks Professor R. E. Kelly for first suggesting that three-dimensional nonlinear critical layers would be scientifically interesting, Professor F. T. Smith for suggesting that the resonant-triad analysis be continued into the fully coupled stage, and his colleague, Dr Sang Soo Lee, for preparing figure 4. The author also thanks his colleagues, Dr Sang Soo Lee, Dr David Wundrow, Dr Lennart Hultgren, Dr Reda Mankbadi and Dr Stewart Leib for their helpful comments during the course of this work.

References

Benney, D. J. & Bergeron, R. F. Jr. 1969 A new class of nonlinear waves in parallel flows. *Stud. Appl. Math.* **48**, 181.

Bodonyi, R. J. & Smith, F. T. 1981 The upper branch stability of the Blasius boundary layer, including non-parallel flow effects. *Proc. R. Soc. Lond.* A **375**, 65–92.

Corke, T. C. & Mangano, R. A. 1989 Resonant growth of three-dimensional modes in transitioning Blasius boundary layers. *J. Fluid Mech.* **209**, 93–150.

Craik, A. D. D. 1971 Nonlinear resonant instability in boundary layers. *J. Fluid Mech.* **50**, 393.

Goldstein, M. E. 1994 Nonlinear interactions between oblique instability waves on nearly parallel shear flows. *Phys. Fluids* **6**, 724–735.

Goldstein, M. E. & Choi, S. W. 1989 Nonlinear evolution of interacting oblique waves on two-dimensional shear layers. *J. Fluid Mech.* **207**, 97 (see also corrigendum *J. Fluid Mech.* **216**, 659).

Goldstein, M. E. & Durbin, P. A. 1986 Nonlinear critical layers eliminate the upper branch of spatially growing Tollmien Schlichting waves. *Phys. Fluids* **29**, 2344.

Goldstein, M. E., Durbin, P. A. & Leib, S. J. 1987 Roll-up of vorticity in adverse-pressure-gradient boundary layers. *J. Fluid Mech.* **183**, 325.

Goldstein, M. E. & Hultgren, L. S. 1988 Nonlinear spatial evolution of an externally excited instability wave in a free shear layer. *J. Fluid Mech.* **197**, 295.

Goldstein, M. E. & Lee, S. S. 1992 Fully coupled resonant-triad interaction in an adverse-pressure-gradient boundary layer. *J. Fluid Mech.* **245**, 523.

Goldstein, M. E. & Lee, S. S. 1993 Oblique instability waves in nearly parallel shear flows. In *Nonlinear waves and weak turbulence with applications in oceanography and condensed matter physics* (ed. N. Fitzmaurice, D. Gurarie, F. McCaughan & W. A. Woyczynski), p. 159. Boston, MA: Birkhauser.

Goldstein, M. E. & Leib, S. J. 1988 Nonlinear roll-up of externally excited free shear layers. *J. Fluid Mech.* **191**, 481.

Goldstein, M. E. & Leib, S. J. 1989 Nonlinear evolution of oblique waves on compressible shear layers. *J. Fluid Mech.* **207**, 73.

Goldstein, M. E. & Wundrow, D. 1995 Interactions of oblique instability waves with weak streamwise vortices. *J. Fluid Mech* **284**, 377.

Hall, P. & Seddougui, S. 1989 On the onset of three dimensionality and time dependence in Görtler vortices. *J. Fluid Mech.* **204**, 405–420.

Hama, F. R. & Nutant, J. 1963 Pulsed hydrogen-bubble visualization tecnique used to investigate transition processes in boundary layers in long running-water channels. In *Proc. Heat Transfer and Fluid Mechanics Inst., 16th Ann. Meeting*, pp. 77–93. Stanford, CA: Stanford University Press.

Hickernell, F. I. 1984 Time-dependent critical layers in shear flows on the beta-plane. *J. Fluid Mech.* **142**, 431.

Huerre, P. 1980. The nonlinear stability of a free shear layer in the viscous critical layer regime. *Phil. Trans. R. Soc. Lond.* A **293**, 643.

Huerre, P. 1987. On the Landau constant in mixing layers. *Proc. R. Soc. Lond.* A **409**, 369.

Hultgren, L. S. 1992. Nonlinear spatial equilibration of an externally excited instability wave in a free shear layer. *J. Fluid Mech.* **236**, 497.

Kachanov, Y. S. 1987. On the resonant nature of the breakdown of a laminar boundary layer. *J. Fluid Mech.* **184**, 43–74.

Kachanov, Y. S., Kozlov, V. V. & Levchenko, V. Y. 1977 Nonlinear propagation of a wave in a boundary layer. *Izv. AN SSSR, Mekh. Zhid. i Gaza* N **3**, 49–58 (in Russian).

Kachanov, Y. S., Kozlov, V. V., Levchenko, V. Y. & Ramazanov, M. P. 1985 On Nature of K-breakdown of a laminar boundary-layer, new experimental data. In *Laminar-turbulent transition* (ed. V. V. Kozlov), pp. 61–73. Berlin: Springer.

Kachanov, Y. S. & Levchenko, V. Y. 1984 The resonant interaction of disturbances at laminar-turbulent transition in a boundary layer. *J. Fluid Mech.* **138**, 209–247.

Khokhlov, A. P. 1994*a* The theory of resonance interaction of Tollmien-Schlichting waves. *J. Appl. Mech. Tech. Phys.* **34**, 508–515.

Khokhlov, A. P. 1994*b*. Asymptotic analysis of resonant interactions in a boundary layer. In *Proc. IUTAM Symp. on Nonlinear Instability of Non-parallel Flows* (ed. S. P. Lin & W. R. C. Phillips). Berlin: Springer.

Klebanoff, P. S. & Tidstrom, K. D. 1959. NASA TN D-195.

Klebanoff, P. S., Tidstrom, K. D. & Sargent, L. M. 1962 The three-dimensional nature of boundary-layer instability. *J. Fluid Mech.* **12**, 1–34.

Kovasznay, L. S. G. Komoda, H. & Vasudeva, B. R. 1962 *Proc. Heat Transfer and Fluid Mech. Inst.* pp. 1–26.

Kozlov, V. V. & Levchenko, V. Y. 1988 Laminar-turbulent transition controlled by localized disturbances. In *Turbulence management and relaminarisation* (ed. H. W. Liepmann & R. Narasimha), pp. 249–269. Berlin: Springer.

Landau, L. D. & Lifshitz, E. M. 1987 *Fluid mechanics*, 2nd. edn. New York: Pergamon.

Leib, S. J. 1991 Nonlinear evolution of subsonic and supersonic disturbances on a compressible mixing layer. *J. Fluid Mech.* **224**, 551.

Leib, S. J. & Lee, S. S. 1994. Nonlinear evolution of a pair of oblique instability waves in a supersonic boundary layer. *J. Fluid Mech.* **282**, 339–371.

Lin, C. C. 1957 On the instability of laminar flow and transition to turbulence. In *IUTAM Symp., Freiburg/BR*, p. 144.

Mack, L. M. 1984 Boundary-layer linear stability theory. In *Special course on stability and transition of laminar flow*. AGARD Report No. 709.

Mack, L. M. 1987 Review of linear compressible stability theory. In *Stability of time dependent and spatially varying flows* (ed. D. L. Dwoyer & M. Y. Hussaini). Berlin: Springer.

Mallier, R. & Maslowe, S. A. 1994. Fully coupled resonant-triad interactions in a free shear layer. *J. Fluid Mech.* **275**, 101–121.

Mankbadi, R. R., Wu, X. & Lee, S. S. 1993. A critical-layer analysis of the resonant triad in boundary-layer transition. *J. Fluid Mech.* **256**, 85.

Nayfeh, A. H. 1981 Effect of streamwise vortices on Tollmien–Schlichting waves. *J. Fluid Mech.* **107**, 441–453.

Nayfeh, A. H & Bozatli, A. N. 1979 Nonlinear wave interactions in boundary layers. AIAA-79-1496.

Nayfeh, A. H. & Al-Maaitah, A. 1988 Influence of streamwise vortices on Tollmien–Schlichting waves. *Phys. Fluids* **31**, 3543–3549.

Nishioka, M. Asai, M. & Iida, S. 1980 An experimental investigation of the secondary instability in plane Poiseuille flow. In *Proc. Symp. on Laminar-Turbulent Transition*. IUTAM Meeting, Stuttgart. Berlin: Springer.

Reid, W. H. 1965 The stability of parallel flows. In *Basic developments in fluid dynamics* (ed. M. Holt), p. 249. New York: Academic.

Saric, W. S. & Thomas, A. S. W. 1984 Experiments on the subharmonic route to turbulence in boundary layers. In *Proc. Int. Symp. on Turbulence and Chaotic Phenomena in Fluids, Kyoto, Japan* (ed. T. Tasumi), p. 117. Amsterdam: North Holland.

Shukhman, I. G. 1991. Nonlinear evolution of spiral density waves generated by the instabiilty of shear layers in rotating compressible fluid. *J. Fluid Mech* **233**, 581–612.

Smith, F. T. & Bowles, R. I. 1992 Transition theory and experimental comparisons on (*a*) amplification into streets (*b*) a strongly nonlinear breakup criterion. *Proc. R. Soc. Lond.* A **439**, 163–175.

Smith, F. T. & Stewart, P. A. 1987 The resonant-triad nonlinear interaction in boundary layer transition. *J. Fluid Mech.* **179**, 227–252.

Stewart, P. A. & Smith, F. T. 1987 Three-dimensional instabilities in steady and unsteady non-parallel boundary layers, including effects of Tollmien–Schlichting disturbances and cross flow. *Proc. R. Soc. Lond.* A **409**, 229–248.

Stewart, P. A. & Smith, F. T. 1992 Three-dimensional nonlinear blow-up from a nearly planar initial disturbance, in boundary-layer transition: theory and experimental comparisons. *J. Fluid Mech.* **244**, 79–100.

Stuart, J. T. 1960 On the nonlinear mechanics of wave disturbances in stable and unstable parallel flows. Part 1. The basic behaviour in plane Poiseuille flow. *J. Fluid Mech.* **9**, 353.

Watson, J. 1960 On the nonlinear mechanics of wave disturbances in stable and unstable parallel

flows. Part 2. The development of a solution for plane Poiseuille flow and for plane Couette flow. *J. Fluid Mech.* **9**, 371.

Wu, X. 1992 The nonlinear evolution of high frequency resonant-triad waves in an oscillating Stokes layer at high Reynolds number. *J. Fluid Mech.* **245**, 553.

Wu, X. 1993 On critical-layer and diffusion-layer nonlinearity in the three-dimensional stage of boundary-layer transition. *Proc. R. Soc. Lond.* A **443**, 95 106.

Wu, X. 1994 Viscous effects on the fully coupled resonant-triad interactions: an analytical approach. *J. Fluid Mech.* (Submitted.)

Wu, X., Lee, S. S. & Cowley, S. J. 1993 On the weakly nonlinear three-dimensional instability of shear layers to pairs of oblique waves: The Stokes layer as a paradigm. *J. Fluid Mech.* **253**, 681.

Wu, X., Stewart, P. A. & Cowley, S. J. 1994 On the weakly nonlinear development of Tollmien Schlichting wavetrains in boundary layers. *Q. J. Mech. Appl. Math.* (Submitted.)

Wundrow, D., Hultgren, L. S. & Goldstein, M. E. 1994 Interaction of oblique instability waves with a nonlinear plane wave. *J. Fluid Mech* **264**, 343 372.

Wundrow, D. & Goldstein, M. E. 1994 Nonlinear evolution of instability waves in a unidirectional transversely sheared mean flow. NASA TM 106779.